Journal of proteome research

Open Access

pubs.acs.org/jpr

Article

Serum N-Glycomics with Nano-LC-QToF LC-MS/MS Reveals N-Glycan Biomarkers for Glioblastoma, Meningioma, and High-Grade Meningioma

Atit Silsirivanit,*,# Michael Russelle S. Alvarez,# Sheryl Joyce Grijaldo-Alvarez, Riya Gogte, Amnat Kitkhuandee, Nontaphon Piyawattanametha, Wunchana Seubwai, Sukanya Luang, Orasa Panawan, Panupong Mahalapbutr, Kulthida Vaeteewoottacharn, Kanlayanee Sawanyawisuth, Worachart Let-itthiporn, Charupong Saengboonmee, Pichayen Duangthongphon, Kritsakorn Jingjit, Anuchit Pankongsap, Sakda Waraasawapati, Chaiwat Aphivatanasiri, and Carlito B. Lebrilla*

Cite This: *J. Proteome Res.* 2025, 24, 1402−1413

Read Online

ACCESS | Metrics & More | Article Recommendations

ABSTRACT: Alteration of glycosylation in cancer cells leads to the expression of tumor-associated glycans, which can be used as biomarkers for diagnosis and prognostic prediction of diseases. In this study, we used nano-LC-QToF to identify serum N-glycan biomarkers for the detection of brain tumors. We observed an increase in sialylated N-glycans and a decrease in fucosylated N-glycans in the serum of patients with glioblastoma (GBM) and meningioma (MG) compared to healthy individuals. In GBM, a combination of increased serum sialylated N-glycan (6_4_0_2 compound) and decreased fucosylated N-glycan (4_4_1_0 compound) was identified as the most appropriate panel, with an area under the curve (AUC) of 0.8660, 78.95% sensitivity, 84.21% specificity, and 82.89% accuracy. For MG, a combination of decreased 6_6_2_0 and 5_5_2_0 compounds and increased 4_4_1_1 compound achieved an AUC of 0.9260, 82.35% sensitivity, 78.57% specificity, and 80.26% accuracy for diagnosis of MG. Additionally, an increase in 5_5_1_0 and 4_3_0_0 compounds combined with a decrease in 7_7_4_3 was associated with high-grade MG (WHO grades II−III). In conclusion, we identified serum N-glycan profiles associated with brain tumors, highlighting their potential as biomarkers for the diagnosis and prognosis of these diseases.

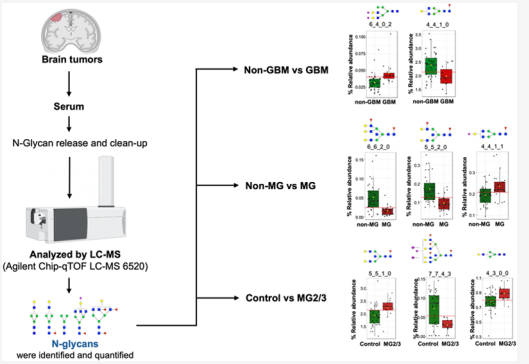

KEYWORDS: *N-glycan, tumor marker, glycosylation, brain tumor, cancer*

1. INTRODUCTION

Brain tumor incidence and mortality are growing rapidly worldwide, driven by factors such as aging, population growth, risk factors, and socioeconomic development. According to GLOBOCAN 2022, the incidence rate for brain tumors is 3.9% (173,591 cases) for males and 3.1% (147,885) for females, while the mortality rate is 3.0% (139,737 cases) for males and 2.2% (108,568 cases) for females.[1] Brain cancers include several types, notably glioblastomas and meningiomas.[2] Glioblastomas are the most aggressive malignant brain tumors, arising from glial cells. On the other hand, meningiomas, which form from the arachnoid cap cells of the brain and spinal cord, are usually benign at first, but often become more aggressive over time.[3] Based on the incidence of brain tumors in the US, glioblastoma is the most common malignant brain tumor, accounting for 48.6%. Among benign brain tumors, meningioma is the most common and pituitary tumor is the second most common, accounting for 53.9 and 24.0%, respectively.[4] Typical diagnostic methods for brain tumors involve neuroimaging and pathological analysis, but definitive diagnoses are made through histological examination.[5]

Tumor cells display a wide range of glycosylation alterations than normal cells.[6] Glycosylation, the addition of glycans to proteins and lipids, occurs in the endoplasmic reticulum (ER) or Golgi apparatus. This process is mediated by enzymes, i.e., glycosyltransferases and glycosidases, which depend on factors including protein substrate bioavailability, enzyme activity, altered enzyme location within subcellular components, and levels of gene transcription.[7] Differential expression of glycosylation enzymes between healthy cells and cancer cells

Received: December 9, 2024
Revised: January 21, 2025
Accepted: January 28, 2025
Published: February 5, 2025

highlights targeting of enzymes involved in the biosynthesis of aberrant glycans in discovering anticancer drugs. Two principal mechanisms contribute to tumor-associated glycans: incomplete synthesis and neo-synthesis.[8] During the early stages of cancer, incomplete synthesis disrupts normal synthesis of complex glycans expressed in epithelial cells, leading to the biosynthesis of truncated structures such as sialyl Tn (STn).[9] In advanced stages, neo-synthesis involves cancer-associated genes that drive the expression of glycan cancer biomarkers like sialyl Lewis^a (SLe^a) and sialyl Lewis^x (SLe^x).[10,11] Several cancer-associated glycosylation changes such as β1,6 branching, sialyl Lewis antigens, α2,6-sialylated lactosamine, T, Tn, and STn antigens, and gangliosides/glycosphingolipids have also been documented.[12]

Liquid chromatography with tandem mass spectrometry (LC-MS/MS)-based methods for the identification of serum glycan biomarkers for cancer have been demonstrated previously, with methods focusing N-glycan using nano-LC-QToF[13−15] and glycopeptides using UPLC-QqQ[13,16−18] mass spectrometry. For example, the N-glycans, $Hex_4HexNac_5Fuc_1$, and $Hex_5HexNAc_6Fuc_1$, as well as the sugar composition signatures, NeuAc2 and Gal4 were found to be biomarkers for lung cancer (AUC = 0.74, 95% CI: 0.68−0.80).[13] In a separate study, a panel of N-glycans—$Hex_6HexNAc_5NeuAc_1$, $Hex_6HexNAc_5NeuAc_3$, $Hex_6HexNAc_5Fuc_2NeuAc_1$, $Hex_7HexNAc_6Fuc_1NeuAc_3$, $Hex_4HexNAc_3NeuAc_1$, and $Hex_5HexNAc_4Fuc_1NeuAc$—were found to be biomarkers for nonsmall cell lung carcinoma (AUC = 0.959, 95% CI: 0.85−1.0).[13]

In this study, we employed nano-LC-QToF N-glycomics to identify N-glycan biomarkers in patients with GBM and MG. In the training data sets, we identified N-glycan structures that were significantly different between brain tumor types. We then constructed biomarker models from this panel of N-glycan structures using logistic regression modeling. These biomarker models were validated for their predictive accuracy using a test data set and were found to perform better as an effective diagnostic tool for brain tumors.

2. MATERIALS AND METHODS

2.1. Ethical Statement and Clinical Sample Collection

The research study was approved by the Human Ethics Committee of Khon Kaen University, Thailand, in accordance with the Declaration of Helsinki and the ICH Good Clinical Practice Guidelines (HE651186). Prior to recruitment, informed consent was obtained from the research participants or their guardians. Brain tumor patients were diagnosed via histopathological analysis at the Department of Pathology, Srinagarind Hospital, Khon Kaen University, Thailand. Serum samples were obtained from the patients with glioblastoma (GBM, n = 19), meningioma (MG, n = 34), and pituitary tumor (PT, n = 3). Control serum samples were obtained from healthy individuals (n = 20) who presented with a normal range of fasting blood sugar, liver function test (aspartate aminotransferase, alanine transaminase, and alkaline phosphatase), and complete blood counts. Detailed clinical and demographic information for the cohort is provided in Table 1.

Table 1. Demographic Data of Brain Tumor Patients and Healthy Controls

	number (n)	age (average, years)	sex (n)	
			male	female
healthy (HE)	20	52.3	11	9
meningioma (MG)	34	50.9	13	21
WHO-Grade I	14	50.8	4	10
WHO-Grade II	17	49.7	6	11
WHO-Grade III	3	60.0	3	0
pituitary tumor (PT)	3	54.7	3	0
glioblastoma multiforme (GBM)	19	54.6	12	7

2.2. Serum N-Glycan Sample Preparation for N-Glycomic Analysis

Serum N-glycans for mass spectrometry analysis were prepared following a previously established protocol.[13,19] Briefly, 25 μL (μL) of serum were reconstituted with 100 μL of PNGase F release buffer (100 mM NH_4CO_3, 5 mM dithiothreitol) and then heated in a 100 °C water bath for 2 min (10 s on, 10 s off). After cooling down to room temperature, 2 μL of PNGase F solution (New England Biolabs) were added to each serum sample and followed by incubation at 37 °C for 18 h. After overnight incubation, the samples were centrifuged at 42,000 rpm (4 °C) for 45 min. The supernatant, containing the released N-glycan and salts, was cleaned-up using solid-phase extraction with porous graphitized carbon (PGC) plates. Purified N-glycans were eluted from the PGC plates using 40% acetonitrile (ACN) containing 0.05% trifluoroacetic acid (TFA) and the solvents were removed *in vacuo* prior to nano-LC-QToF analysis.

2.3. N-Glycomic Nano-LC-QToF Data Acquisition and Analysis

Purified serum N-glycans and quality control samples (prepared from released N-glycans from 6 μg RNase B and 6 μg standard serum solution) were reconstituted in 60 μL ultrapure water and 5 μL were injected into an Agilent 6520 nano-LC-QToF mass spectrometer (Agilent). Separation was performed using an Agilent PGC-Chip II equipped with a 40 nL enrichment column and a 43 mm × 75 μm analytical column (particle size 5 μm). The binary solvent system consisted of mobile phase A (3% v/v ACN and 0.1% v/v formic acid in water) and mobile phase B (90% v/v ACN and 1% v/v formic acid in water). Chromatography was carried out using the gradient as follows: 0−2.5 min, 1% B; 2.5−20 min, 16% B; 20−35 min, 58%; 35−40 min, 100% B; 40−50 min, 100% B; and 50.01−65 min, 0% B, with a flow rate of 0.3 μL/min. Tandem mass spectra were acquired following collision-induced dissociation, with spectra acquired at 0.8 s/spectrum in positive ion mode.

Acquired LC-MS/MS data were processed using MassHunter Qualitative Analysis software B.07 (Agilent) using the "Find by Molecular Feature" algorithm to identify N-glycan compositions from an in-house library of human N-glycans using a quality score of at least 30 and mass accuracy within 10 ppm. To further validate the identified structures, we manually annotated the corresponding MS/MS spectra were manually annotated. N-glycan quantification was carried out by measuring the chromatographic peak area of validated N-glycans from the extracted ion chromatograms in MassHunter, normalized to the total ion chromatogram. N-glycan compounds were annotated as based on their composition: $Hex_aHexNAc_bFuc_cNeuAc_d$, where Hex_a refers to the number of hexose (i.e., mannose, galactose), $HexNAc_b$ refers to the number of *N*-acetylhexosamine (i.e., *N*-acetylglucosamine), Fuc_c refers to the number of fucose, and $NeuAc_d$ refers to the

https://doi.org/10.1021/acs.jproteome.4c01090
J. Proteome Res. 2025, 24, 1402−1413

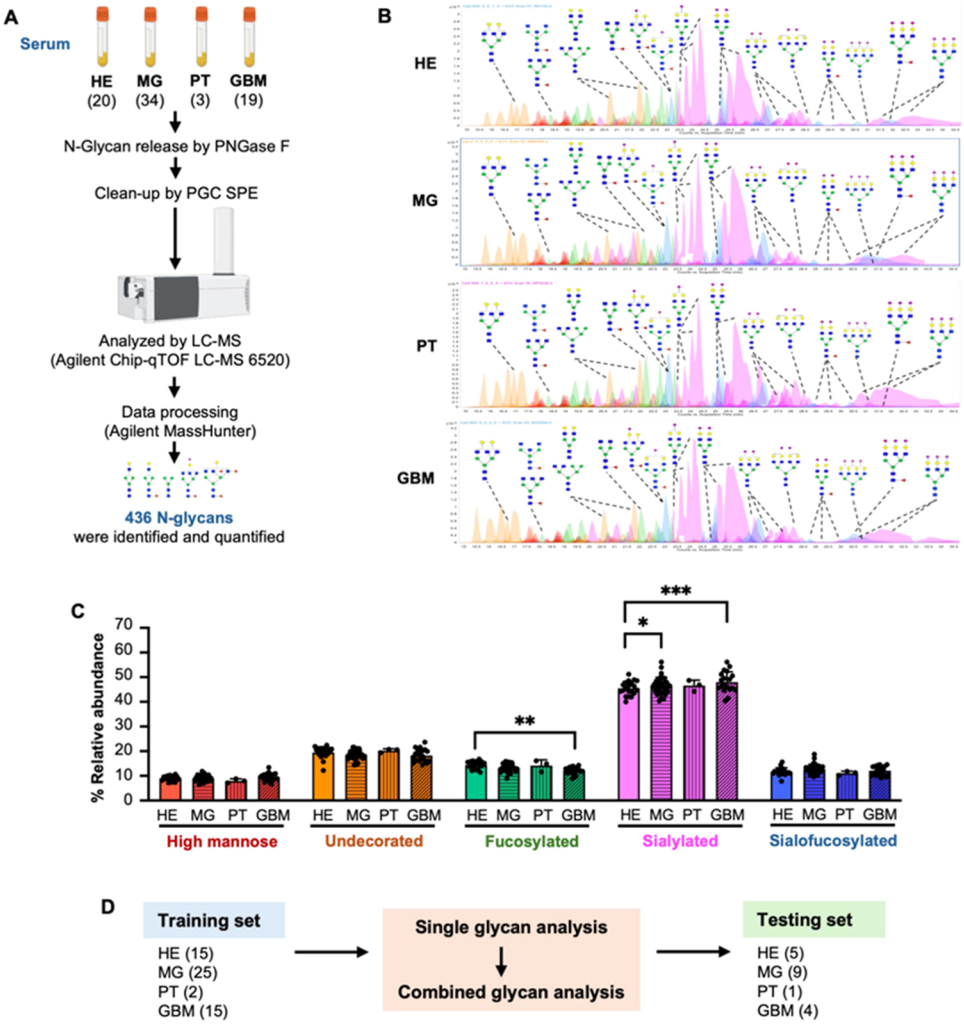

Figure 1. Serum N-glycomics of brain tumor patients. (A) Study design and workflow for serum N-glycomic biomarker analysis of brain tumor patients, meningioma (MG), pituitary tumor (PT), and glioblastoma (GBM) compared to healthy controls (HE). (B) Representative chromatograms of sera collected from HE controls and MG, PT, and GBM cancer patients. (C) Comparison of N-glycan abundances according to N-glycan types between groups. (D) Statistical treatment of training and testing sets for biomarker analysis.

number of neuraminic acid (i.e., sialic acid) residues. N-glycans were subsequently classified using the following classification system: high-mannose ($Hex_aHexNAc_b$, where $b = 2$ denotes the chitobiose core and "a" refers solely to mannose residues), undecorated ($Hex_aHexNAc_b$, where "a" refers to both mannose and galactose residues), fucosylated ($Hex_aHexNAc_bFuc_c$, where $c \geq 1$), sialylated ($Hex_aHexNAc_bNeuAc_d$, where $d \geq 1$), or sialofucosylated ($Hex_aHexNAc_bFuc_cNeuAc_d$, where both c and $d \geq 1$).

2.4. Statistical Analysis

Two-way ANOVA ($\alpha = 0.05$) was performed to compare the abundance of N-glycan compositions and types (high-mannose, undecorated, fucosylated, sialylated, sialofucosylated) followed by Tukey's posthoc test (GraphPad Prism, v. 10.2.3).

Biomarker analysis was performed using MetaboAnalyst 6.0.[20] Processed N-glycan abundance values per category, healthy (HE), meningioma (MG), pituitary tumor (PT), and glioblastoma (GBM), were uploaded to MetaboAnalyst 6.0 and then analyzed using univariate and multivariate ROC analyses. Univariate ROC analysis was obtained using the "Classical univariate ROC curve analyses" module to calculate the ROC curves for individual N-glycan compounds. Multivariate ROC analysis was conducted using the "ROC curve-based model evaluation (Tester)" module, to identify the top ten most important glycan features according to VIP scoring method. To further optimize the model in achieving the best AUC, the most important glycan features with high univariate ROC analysis curves were used in developing the model, as determined by the logistic regression (LR) algorithm. The LR algorithm was used to construct the LR biomarker model from selected N-glycan features.

3. RESULTS

3.1. Serum N-Glycans are Different among Patients with Brain Tumor and Healthy Controls

N-Glycans obtained from the sera of patients with brain tumors (34 meningioma, 19 glioblastoma, and 3 pituitary tumor) and healthy individuals ($n = 20$) were subjected to the LC-MS/MS N-glycomics method, quantifying more than 400 N-glycan compounds (Figure 1A,B). Analysis of N-glycan abundances revealed that the sera were primarily composed of sialylated N-glycans (>40%) (Figure 1C). Statistical comparison of N-glycan abundances classified by type (high-mannose,

https://doi.org/10.1021/acs.jproteome.4c01090
J. Proteome Res. 2025, 24, 1402−1413

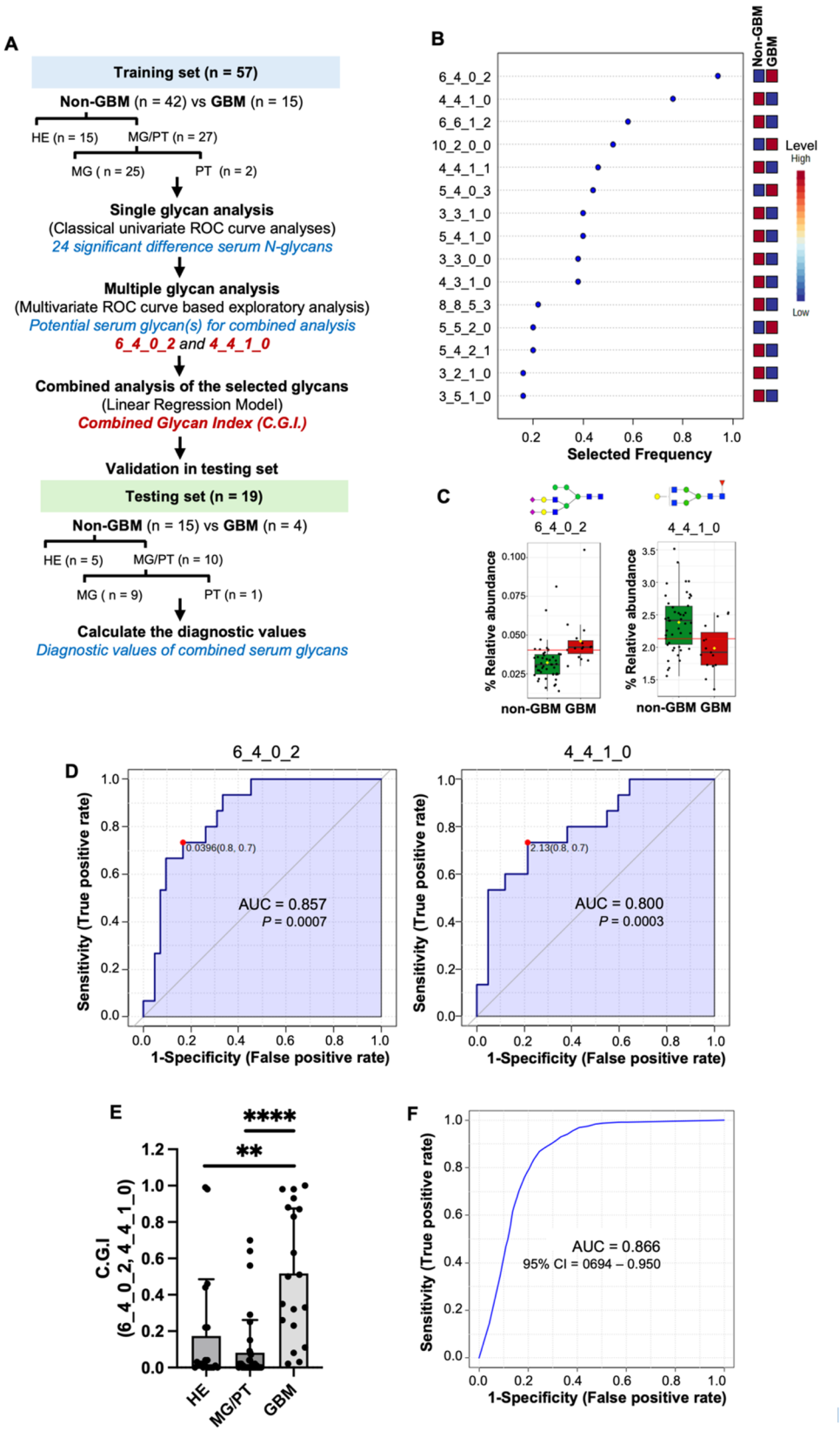

Figure 2. Serum N-glycomics for the diagnosis of glioblastoma (GBM). (A) Study design and statistical treatment for identifying N-glycan biomarkers for the detection of GBM. (B) Importance plot of the top 10 N-glycans for identifying GBM. (C) Comparison of 6_4_0_2 (overexpressed in GBM) and 4_4_1_0 (underexpressed in GBM). (D) Univariate ROC curve analyses of 6_4_0_2 and 4_4_1_0. (E) Comparison of CGI_{GBM} values derived from 6_4_0_2 and 4_4_1_0, between HE, non-GBM (MG, PT), and GBM. (F) Multivariate ROC curve analysis of the combined models of 6_4_0_2 and 4_4_1_0.

https://doi.org/10.1021/acs.jproteome.4c01090
J. Proteome Res. 2025, 24, 1402−1413

Table 2. Top 10 Serum N-Glycans in Glioblastoma (GBM), Meningioma (MG), and High-Grade Meningioma (MG2/3)

no	glycan types	AUC	*P*	$\log_2$ ratio of glycan (control/case)	glycan level in case vs control	cut-off values
			non-GBM (control) vs GBM (case)			
1	6_4_0_2	0.8571	0.0007	−0.58	increased	0.040
2	4_4_1_0	0.8000	0.0003	0.29	decreased	2.130
3	10_2_0_0	0.7730	0.0003	−0.47	increased	0.196
4	6_6_1_2	0.7683	0.0116	1.17	decreased	0.005
5	3_3_0_0	0.7460	0.0123	0.15	decreased	0.253
6	4_4_1_1	0.7349	0.0044	0.33	decreased	0.198
7	3_3_1_0	0.7349	0.0088	0.24	decreased	0.255
8	5_4_1_0	0.7333	0.0087	0.20	decreased	1.410
9	4_3_1_0	0.7254	0.0052	0.25	decreased	0.268
10	4_4_0_0	0.6937	0.0284	0.17	decreased	0.962
			non-MG (control) vs MG (case)			
1	6_6_2_0	0.8356	0.0001	1.71	decreased	0.024
2	5_5_2_0	0.8200	0.0000	0.87	decreased	0.124
3	5_6_0_0	0.7475	0.0040	3.62	decreased	0.009
4	6_6_3_0	0.7369	0.0017	2.52	decreased	0.001
5	4_4_1_1	0.7263	0.0029	−0.29	increased	0.208
6	6_3_1_1	0.7250	0.0068	−0.70	increased	0.011
7	8_7_0_5	0.7206	0.0026	−1.66	increased	0.010
8	4_3_1_1	0.7175	0.0035	−0.30	increased	0.122
9	6_6_1_2	0.7163	0.0050	−0.89	increased	0.013
10	8_8_0_5	0.6863	0.0013	1.67	decreased	0.009
			non-MG + MG grade I (control) vs MG grade II−III (case)			
1	5_5_1_0	0.7778	0.0064	−0.23	Increased	2.179
2	7_7_4_3	0.7651	0.0007	1.27	decreased	0.054
3	4_3_0_0	0.7587	0.0029	−0.20	increased	0.818
4	6_5_1_0	0.7556	0.0008	−0.48	increased	0.182
5	5_4_0_2	0.7524	0.0203	0.18	decreased	14.010
6	6_4_0_0	0.7508	0.0045	−0.25	increased	0.110
7	7_4_0_0	0.7460	0.0057	2.77	decreased	0.003
8	5_4_1_2	0.7444	0.0130	0.29	decreased	2.297
9	7_7_4_4	0.7349	0.0002	−1.85	increased	0.006
10	5_5_1_1	0.7286	0.0216	−0.19	increased	2.825

Table 3. Diagnostic Values of Significantly Different Serum N-Glycans[a]

			diagnostic values (%)						
glycans	AUC	cut-off	sense	spec	PPV	NPV	FP	FN	Acc
			non-GBM vs GBM						
6_4_0_2	0.8571	>0.039	78.95	77.19	53.57	91.67	22.81	21.05	77.63
4_4_1_0	0.8000	<2.130	68.42	82.46	56.52	88.68	17.54	31.58	78.95
			C.G.I = *P*; $\log P/(1\text{-}P) = 2.924 + 54.227(6\_4\_0\_2) - 2.71(4\_4\_1\_0)$						
C.G.I	0.8660	>0.230	78.95	84.21	62.50	92.31	15.79	21.05	82.89
			non-MG vs MG						
6_6_2_0	0.8356	<0.024	82.35	76.19	73.68	84.21	23.81	17.65	78.95
5_5_2_0	0.8200	<0.124	76.47	66.67	65.00	77.78	33.33	23.53	71.05
4_4_1_1	0.7263	>0.208	73.53	61.90	60.98	74.29	38.10	26.47	67.11
			C.G.I = *P*; $\log P/(1\text{-}P) = -0.323 - 79.468(6\_6\_2\_0) + 24.02(4\_4\_1\_1) - 25.119(5\_5\_2\_0)$						
C.G.I	0.9260	>0.410	82.35	78.57	75.68	84.62	21.43	17.65	80.26
			non-MG + MG grade I vs MG grade II & III						
5_5_1_0	0.7778	<0.124	65.00	71.43	44.83	85.11	28.57	35.00	69.74
7_7_4_3	0.7651	<0.024	95.00	51.79	41.30	96.67	48.21	5.00	63.16
4_3_0_0	0.7587	>0.208	80.00	58.93	41.03	89.19	41.07	20.00	64.47
			C.G.I = *P*; $\log P/(1\text{-}P) = -13.677 + 1.686(5\_5\_1\_0) - 39.046(7\_7\_4\_3) + 12.749(4\_3\_0\_0)$						
C.G.I	0.8680	>0.360	70.00	82.14	58.33	88.46	17.86	30.00	78.95

[a]Sensitivity, sense; specificity, spec; positive predictive value, PPV; negative predictive value, NPV; false positive, FP; false negative, FN; accuracy, Acc.

undecorated, fucosylated, sialylated, and sialofucosylated) revealed significant differences in the abundance of fucosylated and sialylated compounds. Specifically, the total abundance of fucosylated compounds was significantly lower in glioblastoma

https://doi.org/10.1021/acs.jproteome.4c01090
J. Proteome Res. 2025, 24, 1402−1413

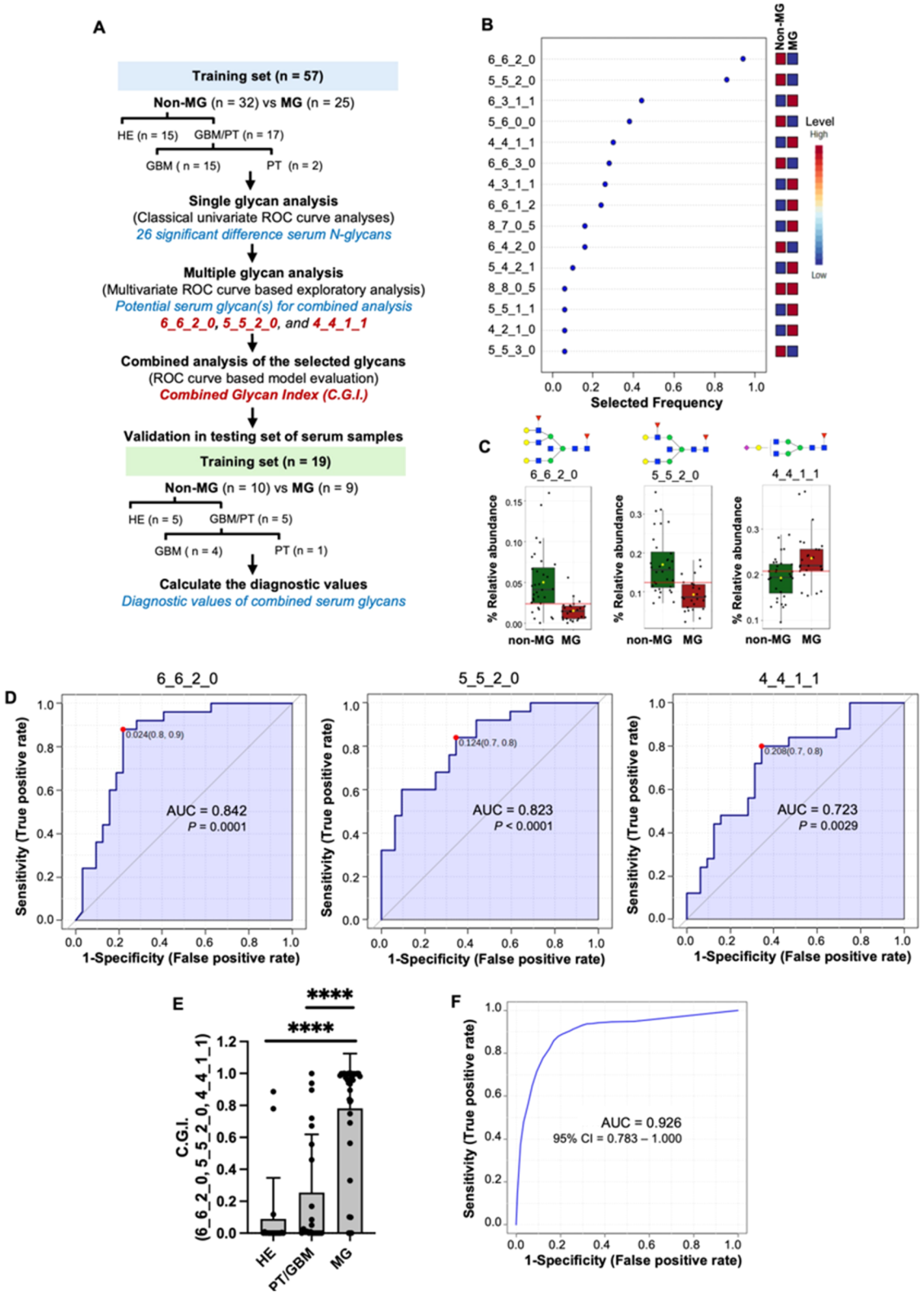

Figure 3. Serum N-glycomics for the diagnosis of meningioma (MG). (A) Study design and statistical treatment for identifying N-glycan biomarkers for the detection of MG. (B) Importance plot of the top 10 N-glycans for identifying MG. (C) Comparison of 4_4_1_1 (overexpressed in MG), and 6_6_2_0 and 5_5_2_0 (underexpressed in MG). (D) Univariate ROC curve analyses of 6_6_2_0, 5_5_2_0, and 4_4_1_0. (E) Comparison of CGI_{MG} values derived from 6_6_2_0, 5_5_2_0, and 4_4_1_0, between HE, non-MG (GBM, PT), and MG. (F) Multivariate ROC curve analysis of the combined model of 6_6_2_0, 5_5_2_0, and 4_4_1_0.

patients compared with healthy controls (p = 0.0036). On the other hand, the total abundance of sialylated compounds was significantly higher in glioblastoma (p = 0.0033) and meningioma (p = 0.0130) patients compared to healthy individuals. Based on these results, further statistical tests were performed to construct biomarker models for glioblastoma and

https://doi.org/10.1021/acs.jproteome.4c01090
J. Proteome Res. 2025, 24, 1402−1413

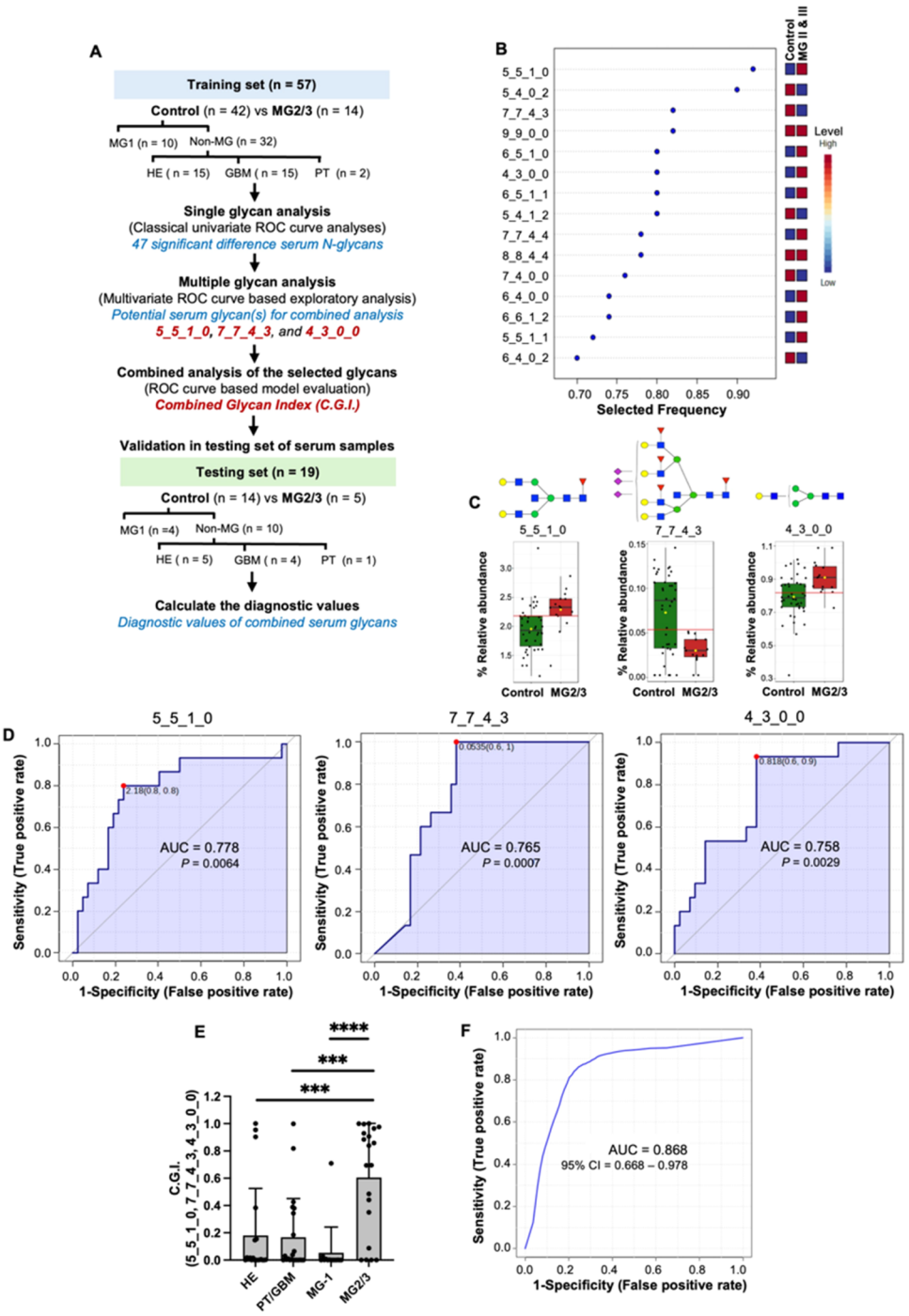

Figure 4. Serum N-glycomics for diagnosis of high-grade meningioma (WHO grades II and III; MG2/3). (A) Study design and statistical treatment for identifying N-glycan biomarkers for the detection of MG2/3. (B) Importance plot of the top 10 N-glycans for identifying MG2/3. (C) Comparison of 5_5_1_0 and 4_3_0_0 (overexpressed in MG2/3), and 7_7_4_3 (underexpressed in MG2/3). (D) Univariate ROC curve analyses of 5_5_1_0, 4_3_0_0, and 7_7_4_3. (E) Comparison of $CGI_{MG2/3}$ values derived from 5_5_1_0, 4_3_0_0, and 7_7_4_3, between HE, non-MG (GBM, PT), MG1 and MG2/3. (F) Multivariate ROC curve analysis of the combined models of 5_5_1_0, 4_3_0_0, and 7_7_4_3.

meningioma by dividing the data sets into training and testing sets in MetaboAnalyst (Figure 1D).

3.2. Sialylated and Fucosylated Serum N-Glycan Biomarkers for the Detection of Glioblastoma

We first constructed biomarker models for glioblastoma (GBM) patients. From the training set (n = 57), non-GBM samples (composed of HE, MG, and PT; n = 42) were separated from GBM samples (n = 15), and N-glycan biomarkers were identified by using ROC curve analyses (Figure 2A). Classical univariate ROC analyses using MetaboAnalyst revealed 2 significantly overexpressed N-glycans in GBM: 6_4_0_2 (p = 0.0007) and 10_2_0_0 (p = 0.0003) (Figure 2B and Table 2). Conversely, the following compounds were underexpressed in GBM: 4_4_1_0 (p = 0.0003), 6_6_1_2 (p = 0.0116), 3_3_0_0 (p = 0.0123), 4_4_1_1 (p = 0.0044), 3_3_1_0 (p = 0.0088), 5_4_1_0 (p = 0.0087), 4_3_1_0 (p = 0.0052), and 4_4_0_0 (p = 0.0284) (Figure 2B andTable 2).

https://doi.org/10.1021/acs.jproteome.4c01090
J. Proteome Res. 2025, 24, 1402−1413

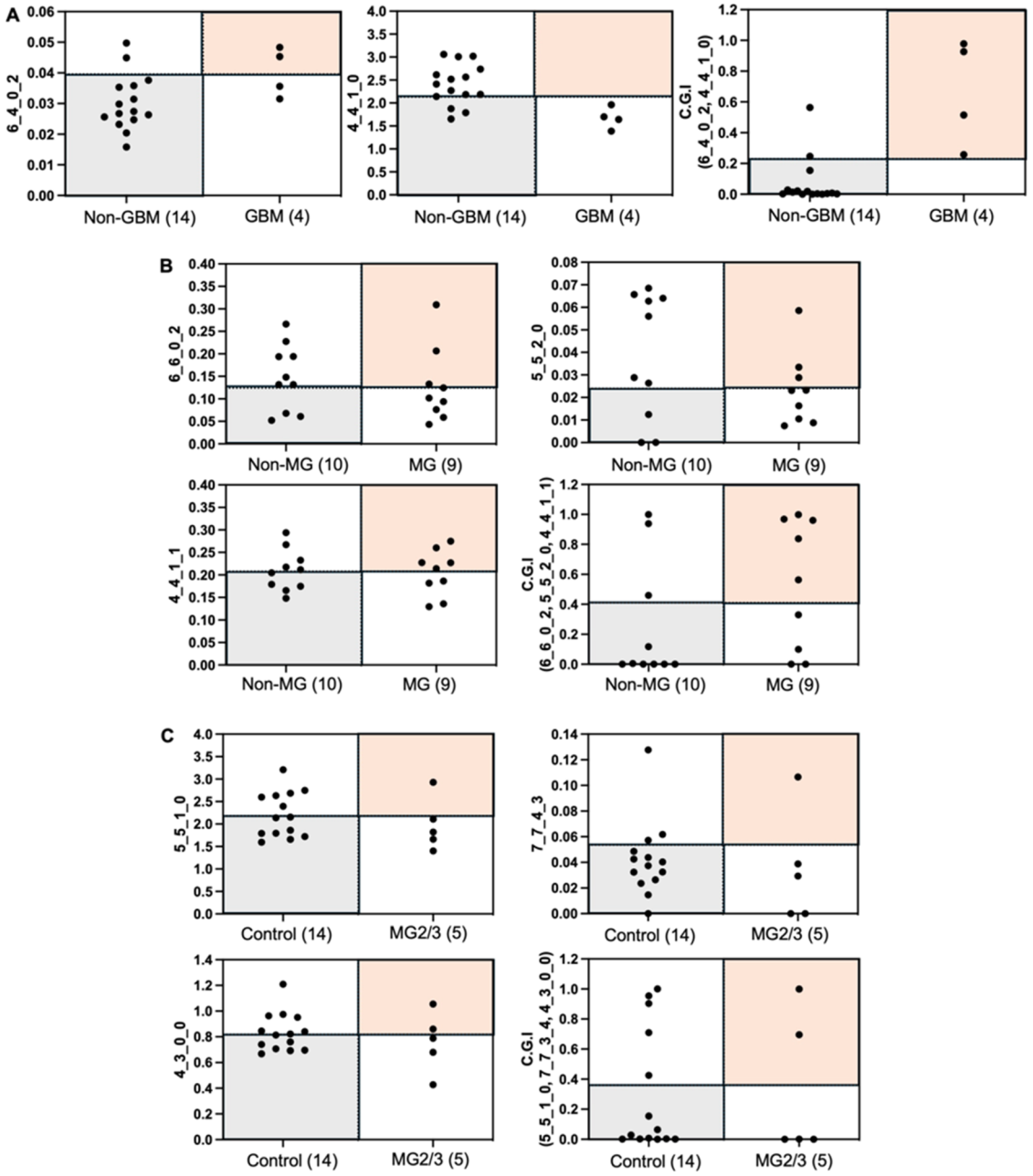

Figure 5. Detection of serum N-glycans in testing sets for GBM (A), MG (B), and MG2/3 (C).

From these significantly expressed N-glycans, 6_4_0_2 (overexpressed) and 4_4_1_0 (underexpressed) provided the best diagnostic performance for GBM versus non-GBM samples, with AUC values of 0.8571 (78.95% sensitivity, 77.19 specificity) and 0.800 (68.42% sensitivity, 82.46% specificity), respectively (Figure 2C,D and Table 3). These two compounds were used to construct a logistic regression (LR) model to determine the combined glycan index (CGI) for GBM

$$\mathrm{CGI}_{\mathrm{GBM}} = P;\ \log\left(\frac{P}{1-P}\right)$$
$$= 2.924 + 54.227(6\_4\_0\_2) - 2.714(4\_4\_1\_0)$$

Calculating the $\mathrm{CGI}_{\mathrm{GBM}}$ for healthy (HE), glioblastoma (GBM), and non-GBM samples showed significantly higher $\mathrm{CGI}_{\mathrm{GBM}}$ value for GBM compared to HE (p = 0.0027) and non-GBM ($p < 0.0001$) (Figure 2E). Furthermore, using the $\mathrm{CGI}_{\mathrm{GBM}}$ with both 6_4_0_2 and 4_4_1_0 improved the diagnostic capability, with an $\mathrm{AUC}_{\mathrm{CGI,GBM}}$ = 0.866 (78.95% sensitivity, 84.21% specificity) (Figure 2F and Table 3). Thus, a serum N-glycan panel of 6_4_0_2 and 4_4_1_0 can be used as biomarkers for the detection of glioblastoma.

3.3. Sialofucosylated and Fucosylated Serum N-Glycan Biomarkers for the Detection of Meningioma

Next, we constructed biomarker models for meningioma (MG) patients. From the training set (n = 57), non-MG samples (composed of HE, GBM, and PT; n = 32) were separated from MG samples (n = 25), and N-glycan biomarkers were identified using ROC curve analyses (Figure 3A). In MetaboAnalyst, we conducted classical univariate ROC analyses to determine the significantly different individual N-glycans and found five compounds to be overexpressed in MG:

https://doi.org/10.1021/acs.jproteome.4c01090
J. Proteome Res. 2025, 24, 1402−1413

4_4_1_1 (p = 0.0029), 6_3_1_1 (p = 0.0068), 8_7_0_5 (p = 0.0026), 4_3_1_1 (p = 0.0035), and 6_6_1_2 (p = 0.0050) (Figure 3B and Table 2). Additionally, five compounds were also significantly underexpressed in MG: 6_6_2_0 (p = 0.0001), 5_5_2_0 (p < 0.0001), 5_6_0_0 (p = 0.0040), 6_6_3_0 (p = 0.0017), and 8_8_0_5 (p = 0.0013) (Figure 3B and Table 2).

Among these, we found that the overexpressed 4_4_1_1 and underexpressed 6_6_2_0 and 5_5_2_0 compounds yielded the best AUC for discriminating between MG and non-MG samples, with AUC values of 0.7263 (73.53% sensitivity, 61.90% specificity), 0.8356 (82.35% sensitivity, 76.19% specificity), and 0.8200 (76.47% sensitivity, 66.67% specificity), respectively (Figure 3C,D and Table 3). These three N-glycans were incorporated to the logistic regression (LR) model for determining the combined glycan index (CGI) for MG

$$\mathrm{CGI_{MG}} = P;\ \log\left(\frac{P}{1-P}\right) = -0.323 - 79.468(6\_6\_2\_0) + 24.02(4\_4\_1\_1) - 25.119(5\_5\_2\_0)$$

Calculating the $\mathrm{CGI_{MG}}$ for healthy (HE), meningioma (MG), and non-MG samples showed significantly higher $\mathrm{CGI_{MG}}$ value for MG compared to HE (p < 0.0001) and non-MG (p < 0.0001) (Figure 3E). Furthermore, using the $\mathrm{CGI_{MG}}$ with the N-glycan panel 6_6_2_0, 5_5_2_0, and 4_4_1_0 improved the diagnostic capability, with an $\mathrm{AUC_{CGI,MG}}$ = 0.9260 (82.35% sensitivity, 78.57% specificity) (Figure 3F and Table 3). Thus, a serum N-glycan panel of 6_6_2_0, 5_5_2_0, and 4_4_1_0 can be used as biomarkers for the detection of meningioma.

3.4. Fucosylated, Sialofucosylated, and Undecorated Serum N-Glycan Biomarkers for the Detection of High-Grade Meningiomas (WHO Grades II and III)

We also constructed biomarker models for high-grade meningioma (MG) patients, specifically WHO grades II and III; from the training set (n = 57), we separated out control samples composed of grade I MG (MG1, n = 10) and non-MG (HE, n = 15; GBM, n = 15; PT, n = 2), from grade II/III MG (MG2/3, n = 14) and then identified N-glycan biomarkers using ROC curve analyses (Figure 4A). In MetaboAnalyst, we conducted classical univariate ROC analyses to determine the significantly different individual N-glycans and found six compounds to be overexpressed in MG2/3:5_5_1_0 (p = 0.0064), 4_3_0_0 (p = 0.0029), 6_5_1_0 (p = 0.0008), 6_4_0_0 (p = 0.0045), 7_7_4_4 (p = 0.0002), and 5_5_1_1 (p = 0.0216) (Figure 4B and Table 2). On the other hand, four compounds were significantly underexpressed in MG2/3:7_7_4_3 (p = 0.0007), 5_4_0_2 (p = 0.0203), 7_4_0_0 (p = 0.0057), and 5_4_1_2 (p = 0.0130) (Figure 4B and Table 2).

From these overexpressed and underexpressed compounds, we found that the overexpressed 5_5_1_0 and 4_3_0_0, and underexpressed 7_7_4_3 compounds yielded the best AUC for discriminating between MG2/3 and control samples, with $\mathrm{AUC_{5\_5\_1\_0}}$ = 0.7778 (65.00% sensitivity, 71.43% specificity), $\mathrm{AUC_{4\_3\_0\_0}}$ = 0.7587 (80.00% sensitivity, 58.93% specificity), and $\mathrm{AUC_{7\_7\_4\_3}}$ = 0.7651 (95.00% sensitivity, 51.79% specificity) (Figure 4C,D and Table 3). Thus, these three compounds were used as an N-glycan panel to construct logistic regression (LR) models for determining the combined glycan index (CGI) of MG2/3

$$\mathrm{CGI_{MG2/3}} = P;\ \log\left(\frac{P}{1-P}\right) = -13.677 - 1.686(5_{5_{1_0}}) - 39.046(7_{7_{4_3}}) + 212.749(4\_3\_0\_0)$$

Calculating the $\mathrm{CGI_{MG2/3}}$ for healthy (HE), non-MG (PT/GBM), meningioma grade I (MG1) and meningioma grades II/III (MG2/3) samples showed significantly higher $\mathrm{CGI_{MG2/3}}$ value for MG2/3 compared to HE (p = 0.0009), non-MG (p = 0.0002), and MG1 (p < 0.0001) (Figure 4E). Furthermore, using the $\mathrm{CGI_{MG2/3}}$ with the N-glycan panel 5_5_1_0, 4_3_0_0, and 7_7_4_3 improved the diagnostic capability, with an $\mathrm{AUC_{CGI,MG2/3}}$ = 0.8680 (70.00% sensitivity, 82.14% specificity) (Figure 4F and Table 3). Thus, a serum N-glycan panel of 5_5_1_0, 4_3_0_0, and 7_7_4_3 can be used as biomarkers for the detection of high-grade meningioma (WHO grades II and III).

3.5. Combined Serum N-Glycans for the Improved Detection of Brain Tumors—Glioblastoma, Meningioma, and High-Grade Meningioma

After the construction and validation of biomarkers for glioblastoma ($\mathrm{AUC_{CGI,GBM}}$ = 0.866), meningioma ($\mathrm{AUC_{CGI,MG}}$ = 0.9260), and high-grade meningioma ($\mathrm{AUC_{CGI,MG2/3}}$ = 0.8680), we tested the models for disease prediction in a training set (Figure 5).

In the GBM testing set (non-GBM n = 14; GBM n = 4), we validated that indeed the abundance of the compound 6_4_0_2 (p = 0.0322) was significantly higher in GBM while 4_4_1_0 (p = 0.0031) was significantly lower, while the $\mathrm{CGI_{GBM}}$ of GBM samples were significantly higher than non-GBM samples (p < 0.0001) (Figure 5A).

In the MG testing set (non-MG n = 10; MG n = 9), we found no statistical significance between the non-MG and MG samples for the abundances of 6_6_2_0 (p = 0.2925) and 4_4_1_1 (p = 0.4057). However, compound 5_5_2_0 was significantly lower in MG than in non-MG samples (p = 0.0870). Similarly, the $\mathrm{CGI_{MG}}$ of MG samples were significantly higher than non-MG samples (p = 0.0832) (Figure 5B).

Finally, in the MG2/3 testing set (control n = 14; MG2/3 n = 5), compounds 5_5_1_0 (p = 0.2071), 7_7_4_3 (p = 0.3440), and 4_3_0_0 (p = 0.2159) were not significantly different in abundance between MG2/3 and control samples. Likewise, the $\mathrm{CGI_{MG2/3}}$ of the control and MG2/3 samples were not significantly different (Figure 5C).

4. DISCUSSION

Aberrant glycosylation has been previously linked with brain cancer pathology.[21−23] Several glycan vaccines, targeting glycosphingolipids, glycoproteins, and proteoglycans, have been developed for tumor immunotherapy. For glycoproteins, the T^n, ST^n, and TF antigens have been reportedly overexpressed in several cancer types including brain, bladder, colorectal, ovarian, and breast.[24,25] Identification of circulating markers that are applicable for diagnosis and prognosis is still a challenging task for the management of brain tumors. Currently, no clinically validated circulating biomarkers available for brain tumors, this might be due to blood-brain barrier that restrict the transportation between the brain and

https://doi.org/10.1021/acs.jproteome.4c01090
J. Proteome Res. 2025, 24, 1402−1413

Table 4. Summary and Comparison of Serum N-Glycan Panels for Glioblastoma, Meningioma, and High-Grade Meningioma

Brain tumor	Serum N-glycan panel	Expression level (tumor/control)	Model performance (AUC)
Glioblastoma (GBM)	6_4_0_2 	Overexpressed	$AUC_{CGI,GBM}$=0.866
	4_4_1_0 	Underexpressed	
Meningioma (MG)	4_4_1_1 	Overexpressed	$AUC_{CGI,GM}$=0.926
	6_6_2_0 	Underexpressed	
	5_5_2_0 	Underexpressed	
High-grade meningioma (WHO grades II and III; MG2/3)	5_5_1_0 	Overexpressed	$AUC_{CGI,MG2/3}$=0.868
	4_3_0_0 	Overexpressed	
	7_7_4_3 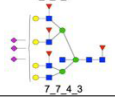	Underexpressed	

blood.[26] Recently, many research groups persevere to identify the circulating markers in the management of brain tumors.[26−28]

With LC-MS/MS N-glycomics, we were able to quantify the differences in serum N-glycan expression between cancer patients and healthy controls at a molecular structural level. As such, we generated a panel of N-glycan compounds for the detection of a specific cancer. We have previously applied this method to ovarian cancer,[18] lung cancer,[13,14] and Alzheimer's disease,[29] and we have applied the method herein for multiple brain cancer types−glioblastoma, meningioma, and high-grade meningioma (Table 4). Due to the pathological differences among these brain tumor types, we observed distinct N-glycan structures in the biomarker discovery panel for each. In glioblastoma, sialylated (6_4_0_2) and fucosylated (4_4_1_0) structures were significantly altered, whereas in meningioma, sialofucosylated (4_4_1_1), and fucosylated (6_6_2_0 and 5_5_2_0) structures were significantly different. Between low-grade meningioma (grade I) and high-grade meningioma (grades II and III), significant differences were observed in undecorated (4_3_0_0), fucosylated (5_5_1_0), and sialofucosylated (7_7_4_3) structures. Notably, some striking differences and similarities emerged in the structures and compositions of these N-glycans. The fucosylated biantennary structure 4_4_1_0 is underexpressed in glioblastoma, but its sialofucosylated counterpart 4_4_1_1 is significantly overexpressed in meningioma sera. The bisecting fucosylated structure 5_5_1_0 is overexpressed in high-grade meningioma, and its diffucosylated counterpart 5_5_2_0 is underexpressed in meningioma. Since changes in N-glycan expression reflect alterations in protein glycosylation machinery, it would be interesting to correlate these findings with glycoproteomics data to determine the serum glycoproteins bearing these distinct N-glycan structures in brain tumor patients.

Similar to our study, the data previously presented by Varadi et al. showed that sialylated N-glycans were elevated in the serum of glioblastoma and meningioma patients compared to healthy controls.[30] Increased sialylation in cancer cells and serum was associated with disease progression and poor clinical outcomes in cancer patients.[31−34] Additionally, sialylation has been implicated in the survival of glioblastoma stem cells.[35] Identifying and targeting the sialyltransferase enzymes associated with glioblastoma and meningioma could provide an alternative treatment approach for the diseases. Furthermore, a decrease in core-fucosylated N-glycan in the serum of glioblastoma and meningioma patients has also been demonstrated;[30] this information suggests an alteration in core-fucosylation in brain tumors, particularly glioblastoma and meningioma. Further functional studies of core-fucosylation in brain tumors are warranted. Moreover, to enhance the efficiency of disease detection, the serum N-glycoproteins that carry these glycans should be further characterized. This information may deepen our understanding of the tumor biology of glioblastoma and meningioma.

5. CONCLUSIONS

In summary, we utilized nano-LC-QToF N-glycomics methods to identify significantly different N-glycan compounds in the sera of patients that can be used as biomarkers for the detection of glioblastoma and meningioma.

■ ASSOCIATED CONTENT

Data Availability Statement

Raw and processed LC-MS/MS data are available at the MassIVE database (doi:10.25345/C5N58CZ1R; MSV000096282).

■ AUTHOR INFORMATION

Corresponding Authors

Atit Silsirivanit − *Department of Biochemistry, Faculty of Medicine, Khon Kaen University, Khon Kaen 40002, Thailand;* orcid.org/0000-0002-5777-3843; Phone: +66-43-363-265; Email: atitsil@kku.ac.th

Carlito B. Lebrilla − *Department of Chemistry, University of California, Davis, Davis, California 95616, United States;* orcid.org/0000-0001-7190-5323; Phone: +1-530-752-6364; Email: cblebrilla@ucdavis.edu

Authors

Michael Russelle S. Alvarez − *Department of Chemistry, University of California, Davis, Davis, California 95616, United States;* orcid.org/0000-0001-6411-9906

https://doi.org/10.1021/acs.jproteome.4c01090
J. Proteome Res. 2025, 24, 1402−1413

Sheryl Joyce Grijaldo-Alvarez − *Department of Chemistry, University of California, Davis, Davis, California 95616, United States*
Riya Gogte − *Department of Chemistry, University of California, Davis, Davis, California 95616, United States*
Amnat Kitkhuandee − *Department of Surgery, Faculty of Medicine, Khon Kaen University, Khon Kaen 40002, Thailand*
Nontaphon Piyawattanametha − *Department of Surgery, Faculty of Medicine, Khon Kaen University, Khon Kaen 40002, Thailand*
Wunchana Seubwai − *Department of Forensic Medicine, Faculty of Medicine, Khon Kaen University, Khon Kaen 40002, Thailand*
Sukanya Luang − *Department of Biochemistry, Faculty of Medicine, Khon Kaen University, Khon Kaen 40002, Thailand*
Orasa Panawan − *Department of Biochemistry, Faculty of Medicine, Khon Kaen University, Khon Kaen 40002, Thailand*
Panupong Mahalapbutr − *Department of Biochemistry, Faculty of Medicine, Khon Kaen University, Khon Kaen 40002, Thailand;* orcid.org/0000-0003-4389-334X
Kulthida Vaeteewoottacharn − *Department of Biochemistry, Faculty of Medicine, Khon Kaen University, Khon Kaen 40002, Thailand*
Kanlayanee Sawanyawisuth − *Department of Biochemistry, Faculty of Medicine, Khon Kaen University, Khon Kaen 40002, Thailand*
Worachart Let-itthiporn − *Department of Biochemistry, Faculty of Medicine, Khon Kaen University, Khon Kaen 40002, Thailand*
Charupong Saengboonmee − *Department of Biochemistry, Faculty of Medicine, Khon Kaen University, Khon Kaen 40002, Thailand*
Pichayen Duangthongphon − *Department of Surgery, Faculty of Medicine, Khon Kaen University, Khon Kaen 40002, Thailand*
Kritsakorn Jingjit − *Department of Surgery, Faculty of Medicine, Khon Kaen University, Khon Kaen 40002, Thailand*
Anuchit Pankongsap − *Department of Surgery, Faculty of Medicine, Khon Kaen University, Khon Kaen 40002, Thailand*
Sakda Waraasawapati − *Department of Pathology, Faculty of Medicine, Khon Kaen University, Khon Kaen 40002, Thailand*
Chaiwat Aphivatanasiri − *Department of Pathology, Faculty of Medicine, Khon Kaen University, Khon Kaen 40002, Thailand*

Complete contact information is available at: https://pubs.acs.org/10.1021/acs.jproteome.4c01090

Author Contributions

#A.S. and M.R. contributed equally to this work.

Notes

The authors declare no competing financial interest.

■ ACKNOWLEDGMENTS

This study was funded by the Fundamental Fund of Khon Kaen University. We would like to thank the support from the National Research Council of Thailand (N42A650238) and the Faculty for Medicine, Khon Kaen University for A.S. This study received bio-specimens from Khon Kaen University, Faculty of Medicine and Mekong Health Sciences Research Institute Biobank Project.

■ REFERENCES

(1) Bray, F.; Laversanne, M.; Sung, H.; Ferlay, J.; Siegel, R. L.; Soerjomataram, I.; Jemal, A. Global cancer statistics 2022: GLOBOCAN estimates of incidence and mortality worldwide for 36 cancers in 185 countries. *Ca-Cancer J. Clin.* **2024**, *74* (3), 229−263.
(2) Atallah, O.; Almealawy, Y. F.; Awuah, W. A.; Conti, A.; Chaurasia, B. Is simultaneous occurrence of meningioma and glioblastoma a mere coincidence? *Clin. Neurol. Neurosurg.* **2024**, *236*, No. 108099.
(3) Gajjar, K.; Heppenstall, L. D.; Pang, W.; Ashton, K. M.; Trevisan, J.; Patel, I. I.; Llabjani, V.; Stringfellow, H. F.; Martin-Hirsch, P. L.; Dawson, T.; Martin, F. L. Diagnostic segregation of human brain tumours using Fourier-transform infrared and/or Raman spectroscopy coupled with discriminant analysis. *Anal. Methods* **2013**, *5* (1), 89−102.
(4) Miller, K. D.; Ostrom, Q. T.; Kruchko, C.; Patil, N.; Tihan, T.; Cioffi, G.; Fuchs, H. E.; Waite, K. A.; Jemal, A.; Siegel, R. L.; Barnholtz-Sloan, J. S. Brain and other central nervous system tumor statistics, 2021. *Ca-Cancer J. Clin.* **2021**, *71* (5), 381−406.
(5) Chamberlin, K.; Chamberlin, G.; Saunders, K.; Khagi, S. Next-generation sequencing reveals novel mutations in a collision tumor of glioblastoma and meningioma. *CNS Oncol.* **2021**, *10* (2), No. CNS70.
(6) Pinho, S. S.; Reis, C. A. Glycosylation in cancer: mechanisms and clinical implications. *Nat. Rev. Cancer* **2015**, *15* (9), 540−555.
(7) Reily, C.; Stewart, T. J.; Renfrow, M. B.; Novak, J. Glycosylation in health and disease. *Nat. Rev. Nephrol.* **2019**, *15* (6), 346−366.
(8) Kannagi, R.; Yin, J.; Miyazaki, K.; Izawa, M. Current relevance of incomplete synthesis and neo-synthesis for cancer-associated alteration of carbohydrate determinants—Hakomori's concepts revisited. *Biochim. Biophys. Acta, Gen. Subj.* **2008**, *1780* (3), 525−531.
(9) Munkley, J.; Elliott, D. J. Hallmarks of glycosylation in cancer. *Oncotarget* **2016**, *7*, 35478−35489, DOI: 10.18632/oncotarget.8155.
(10) Cohen, E. N.; Fouad, T. M.; Lee, B.-N.; Arun, B. K.; Liu, D.; Tin, S.; Barrera, A. M. G.; Miura, T.; Kiyokawa, I.; Yamashita, J.; et al. Elevated serum levels of sialyl Lewis X (sLeX) and inflammatory mediators in patients with breast cancer. *Breast Cancer Res. Treat.* **2019**, *176* (3), 545−556.
(11) Liang, J. X.; Liang, Y.; Gao, W. Clinicopathological and prognostic significance of sialyl Lewis X overexpression in patients with cancer: a meta-analysis. *OncoTargets Ther.* **2016**, *9*, 3113−3125.
(12) Dall'Olio, F.; Malagolini, N.; Trinchera, M.; Chiricolo, M. Mechanisms of cancer-associated glycosylation changes. *Front. Biosci.* **2012**, *17* (2), 670−699.
(13) Alvarez, M. R. S.; Zhou, Q.; Tena, J.; Lebrilla, C. B.; Completo, G. C.; Heralde, F. M., 3rd; Cabanatan, M.; Barzaga, M. T.; Tan-Liu, N.; Ladrera, G. I.; et al. N-Glycan and Glycopeptide Serum Biomarkers in Philippine Lung Cancer Patients Identified Using Liquid Chromatography-Tandem Mass Spectrometry. *ACS Omega* **2022**, *7* (44), 40230−40240.
(14) Ruhaak, L. R.; Stroble, C.; Dai, J.; Barnett, M.; Taguchi, A.; Goodman, G. E.; Miyamoto, S.; Gandara, D.; Feng, Z.; Lebrilla, C. B.; Hanash, S. Serum Glycans as Risk Markers for Non−Small Cell Lung Cancer. *Cancer Prev. Res.* **2016**, *9* (4), 317−323.
(15) Ruhaak, L. R.; Taylor, S. L.; Stroble, C.; Nguyen, U. T.; Parker, E. A.; Song, T.; Lebrilla, C. B.; Rom, W. N.; Pass, H.; Kim, K.; et al. Differential N-Glycosylation Patterns in Lung Adenocarcinoma Tissue. *J. Proteome Res.* **2015**, *14* (11), 4538−4549.
(16) Hong, Q.; Ruhaak, L. R.; Stroble, C.; Parker, E.; Huang, J.; Maverakis, E.; Lebrilla, C. B. A Method for Comprehensive Glycosite-Mapping and Direct Quantitation of Serum Glycoproteins. *J. Proteome Res.* **2015**, *14* (12), 5179−5192.

(17) Li, Q.; Kailemia, M. J.; Merleev, A. A.; Xu, G.; Serie, D.; Danan, L. M.; Haj, F. G.; Maverakis, E.; Lebrilla, C. B. Site-Specific Glycosylation Quantitation of 50 Serum Glycoproteins Enhanced by Predictive Glycopeptidomics for Improved Disease Biomarker Discovery. *Anal. Chem.* **2019**, *91* (8), 5433−5445.
(18) Miyamoto, S.; Stroble, C. D.; Taylor, S.; Hong, Q.; Lebrilla, C. B.; Leiserowitz, G. S.; Kim, K.; Ruhaak, L. R. Multiple Reaction Monitoring for the Quantitation of Serum Protein Glycosylation Profiles: Application to Ovarian Cancer. *J. Proteome Res.* **2018**, *17* (1), 222−233.
(19) Li, Q.; Xie, Y.; Wong, M.; Barboza, M.; Lebrilla, C. B. Comprehensive structural glycomic characterization of the glycocalyxes of cells and tissues. *Nat. Protoc.* **2020**, *15* (8), 2668−2704.
(20) Pang, Z.; Lu, Y.; Zhou, G.; Hui, F.; Xu, L.; Viau, C.; Spigelman, A. F.; MacDonald, P. E.; Wishart, D. S.; Li, S.; Xia, J. MetaboAnalyst 6.0: towards a unified platform for metabolomics data processing, analysis and interpretation. *Nucleic Acids Res.* **2024**, *52*, W398−W406, DOI: 10.1093/nar/gkae253.
(21) Guo, Y.; Jia, W.; Yang, J.; Zhan, X. Cancer glycomics offers potential biomarkers and therapeutic targets in the framework of 3P medicine. *Front. Endocrinol.* **2022**, *13*, No. 970489, DOI: 10.3389/fendo.2022.970489.
(22) Sun, Y.-F.; Zhang, L.-C.; Niu, R.-Z.; Chen, L.; Xia, Q.-J.; Xiong, L.-L.; Wang, T.-H. Predictive potentials of glycosylation-related genes in glioma prognosis and their correlation with immune infiltration. *Sci. Rep.* **2024**, *14* (1), No. 4478.
(23) Yue, J.; Huang, R.; Lan, Z.; Xiao, B.; Luo, Z. Abnormal glycosylation in glioma: related changes in biology, biomarkers and targeted therapy. *Biomarker Res.* **2023**, *11* (1), No. 54.
(24) Freitas, R.; Relvas-Santos, M.; Azevedo, R.; Soares, J.; Fernandes, E.; Teixeira, B.; Santos, L. L.; Silva, A. M. N.; Ferreira, J. A. Single-pot enzymatic synthesis of cancer-associated MUC16 O-glycopeptide libraries and multivalent protein glycoconjugates: a step towards cancer glycovaccines. *New J. Chem.* **2021**, *45* (20), 9197−9211.
(25) Ghosh, S.; Trabbic, K. R.; Shi, M.; Nishat, S.; Eradi, P.; Kleski, K. A.; Andreana, P. R. Chemical synthesis and immunological evaluation of entirely carbohydrate conjugate Globo H-PS A1. *Chem. Sci.* **2020**, *11* (48), 13052−13059.
(26) Zanganeh, S.; Abbasgholinejad, E.; Doroudian, M.; Esmaelizad, N.; Farjadian, F.; Benhabbour, S. R. The Current Landscape of Glioblastoma Biomarkers in Body Fluids. *Cancers* **2023**, *15* (15), No. 3804.
(27) Halabi, R.; Dakroub, F.; Haider, M. Z.; Patel, S.; Amhaz, N. A.; Reslan, M. A.; Eid, A. H.; Mechref, Y.; Darwiche, N.; Kobeissy, F.; et al. Unveiling a Biomarker Signature of Meningioma: The Need for a Panel of Genomic, Epigenetic, Proteomic, and RNA Biomarkers to Advance Diagnosis and Prognosis. *Cancers* **2023**, *15* (22), No. 5339.
(28) Tena, J.; Tang, X.; Zhou, Q.; Harvey, D.; Barajas-Mendoza, M.; Jin, L.-W.; Maezawa, I.; Zivkovic, A. M.; Lebrilla, C. B. Glycosylation alterations in serum of Alzheimer's disease patients show widespread changes in N-glycosylation of proteins related to immune function, inflammation, and lipoprotein metabolism. *Alzheimer's Dementia* **2022**, *14* (1), No. e12309.
(29) Bark, J. M.; Kulasinghe, A.; Chua, B.; Day, B. W.; Punyadeera, C. Circulating biomarkers in patients with glioblastoma. *Br. J. Cancer* **2020**, *122* (3), 295−305.
(30) Váradi, C.; Hajdu, V.; Farkas, F.; Gilányi, I.; Oláh, C.; Viskolcz, B. The Analysis of Human Serum N-Glycosylation in Patients with Primary and Metastatic Brain Tumors. *Life* **2021**, *11* (1), No. 29.
(31) Dobie, C.; Skropeta, D. Insights into the role of sialylation in cancer progression and metastasis. *Br. J. Cancer* **2021**, *124* (1), 76−90.
(32) Munkley, J. Aberrant Sialylation in Cancer: Therapeutic Opportunities. *Cancers* **2022**, *14* (17), No. 4248.
(33) Silsirivanit, A. Glycan and Glycosylation as a Target for Treatment of Glioblastoma. In *Glioblastoma*; Amit, A.; Singh, K. D., Eds.; IntechOpen, 2022.
(34) Wen, R.; Zhao, H.; Zhang, D.; Chiu, C.-L.; Brooks, J. D. Sialylated glycoproteins as biomarkers and drivers of progression in prostate cancer. *Carbohydr. Res.* **2022**, *519*, No. 108598.
(35) Putthisen, S.; Silsirivanit, A.; Panawan, O.; Niibori-Nambu, A.; Nishiyama-Ikeda, Y.; Ma-In, P.; Luang, S.; Ohta, K.; Muisuk, K.; Wongkham, S.; Araki, N. Targeting alpha2,3-sialylated glycan in glioma stem-like cells by Maackia amurensis lectin-II: A promising strategy for glioma treatment. *Exp. Cell Res.* **2022**, *410* (1), No. 112949.

https://doi.org/10.1021/acs.jproteome.4c01090
J. Proteome Res. 2025, 24, 1402−1413